

BAYESIAN COMMUNITY DETECTION FOR NETWORKS WITH COVARIATES

LUYI SHEN¹, ARASH AMINI², NATHANIEL JOSEPHS³, AND LIZHEN LIN¹

ABSTRACT. The increasing prevalence of network data in a vast variety of fields and the need to extract useful information out of them have spurred fast developments in related models and algorithms. Among the various learning tasks with network data, community detection, the discovery of node clusters or “communities,” has arguably received the most attention in the scientific community. In many real-world applications, the network data often come with additional information in the form of node or edge covariates that should ideally be leveraged for inference. In this paper, we add to a limited literature on community detection for networks with covariates by proposing a Bayesian stochastic block model with a covariate-dependent random partition prior. Under our prior, the covariates are explicitly expressed in specifying the prior distribution on the cluster membership. Our model has the flexibility of modeling uncertainties of all the parameter estimates including the community membership. Importantly, and unlike the majority of existing methods, our model has the ability to learn the number of the communities via posterior inference without having to assume it to be known. Our model can be applied to community detection in both dense and sparse networks, with both categorical and continuous covariates, and our MCMC algorithm is very efficient with good mixing properties. We demonstrate the superior performance of our model over existing models in a comprehensive simulation study and an application to two real datasets.

Keywords: Community detection; Networks with covariates; Covariate-dependent random partition prior; Gibbs sampler

1. INTRODUCTION

The ubiquity of network data in modern science and engineering and the need to extract meaningful information out of them has spurred rapid developments in the models, theory, and algorithms for the inference of networks [6, 4, 28, 12, 15, 13]. Among the specific learning tasks with network data, community detection, which aims to detect communities or clusters among nodes, has arguably received the most attention in the scientific community. Various models and algorithms have been developed for community detection in networks including modularity-based methods [19], spectral clustering algorithms [16, 21], stochastic block models [9, 11, 3],

1. Department of Applied and Computational Mathematics and Statistics, The University of Notre Dame

2. Department Statistics, UCLA

3. Department of Biostatistics, Yale School of Public Health

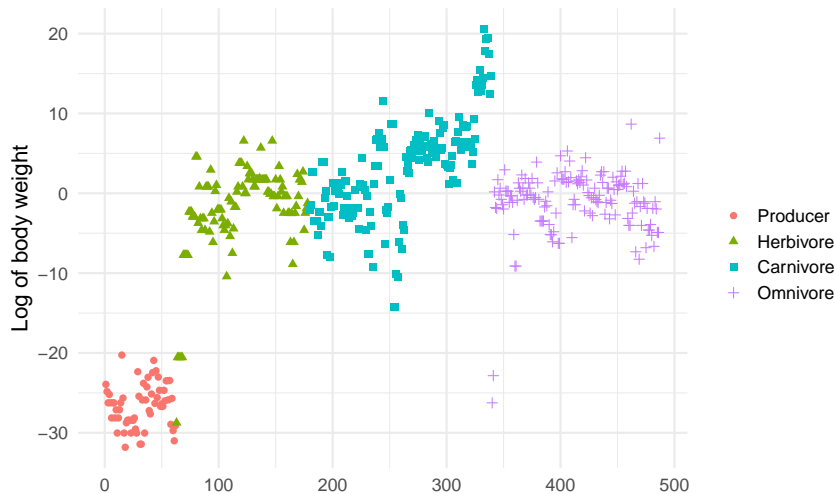


FIGURE 1. Log body mass for different species colored by their feeding type.

optimization-based approaches via semidefinite programming [1], and various Bayesian models [17, 2], among others.

Besides the edge information of an observed network, there are often additional covariates or nodal information available in many real-world networks. These additional covariates should be ideally utilized when performing community detection. For example, in a Facebook network, one can obtain from an individual’s profile covariates including current city, workplace, hometown, education, and hobbies. Another example is the Weddell Sea trophic network, which describes the marine ecosystem of the Weddell Sea [10]. It is a predator-prey network that includes the average adult body mass for each of the species. If one were to only utilize the network information, it is hard to differentiate all the different feeding types. However, the body mass of each species shows a partial clustering by the group, as seen in Figure 1. Therefore, a better clustering should be achievable when both the network and covariates are incorporated.

Such network data have motivated an emerging line of work that aims to deal with community detection problems that leverage both the network and the exogenous covariates. A node-coupled stochastic block model (NSBM) is proposed in [27] in which cluster information or the block matrix is uniquely encoded by the covariates. Another model from [31] specifies that the link probability between a pair of nodes is contributed additively by the block probability in an SBM and a similarity measure between the covariates of a pair of nodes. A similar class of block models is proposed in [25] that also accommodates covariates in an additive way such that the link probability is influenced by both block membership and covariates. A covariate-assisted spectral clustering algorithm is proposed in [5]. Categorical covariates on the

actor level are included in the model in [26], and the block affiliation probabilities are modeled conditional on the covariates via a multinomial probit model. Another prominent method in the frequentist literature is due to [30] in which a joint community detection criterion is proposed using both the adjacency matrix of the network and the node features, and their algorithm weights the edges according to feature similarities. Recently, the interplay between network information and covariates is investigated in an optimization framework for community detection in sparse networks in [29].

We add to this literature by proposing a Bayesian community detection procedure in which the effects of the covariates are incorporated via a covariate-dependent random partition prior on the node labels of a stochastic block model. The covariates are explicitly expressed and incorporated in the prior probability of generating clusters. One of the distinctive features of our models compared with the ones already proposed in the literature is that ours has the ability to learn the number of communities via posterior inference without having to assume it to be known. The proposed model has the flexibility of assessing uncertainties for all the model parameters through an efficient MCMC algorithm for posterior inference.

Our model can be applied in both dense and sparse regimes. In a sparse regime, as one of our simulation studies shows, our model outperforms other state-of-the-art methods such as that of [29], whose primary goal was to deal with sparse network condition with covariates. We also apply our methods to networks that have covariates with relatively high-dimensions. Our extensive simulations demonstrate our overall superior performance over existing methods in networks with continuous or categorical features, even when those methods are given the true number of communities.

The remainder of our paper is organized as follows. Section 2 is devoted to our model description and MCMC algorithms. In Section 3, we carry out several simulation studies in various settings to demonstrate the utility of our proposed model and algorithms. We also apply our model to two data examples in Section 4. We conclude in Section 5 with possibilities for future work.

2. PRIOR, MODEL, AND MCMC ALGORITHM

Consider an observed network on n nodes represented by an $n \times n$ adjacency matrix $A = (A_{ij})$ with $A_{ij} = 1$ indicating the presence of a link between nodes i and j , and $A_{ij} = 0$ otherwise. Assume in addition that we have some covariate information $x_i \in \mathbb{R}^p$ for each node $i = 1, \dots, n$. The covariate information associated with the node are often referred to as nodal information or node features of the network, and are frequently encountered in modern network data. We let $\mathbf{x} = (x_1, \dots, x_n)^T \in \mathbb{R}^{n \times p}$ denote all of the node covariates of a given network. Our goal is to perform network community detection by incorporating both the network structure and the nodal information. The key challenge is how to jointly model these two sources of information. Below we propose a Bayesian model that incorporates the nodal information in the prior probability of cluster membership within an SBM.

Let $\mathbf{z} = (z_1, \dots, z_n) \in \mathbb{N}^n$ be a node membership vector and $L(\mathbf{z}) = \max\{z_i : i \in [n]\}$ indicate the total number of clusters implied by \mathbf{z} . We do not assume $L(\mathbf{z})$ to be known *a priori*. Let $S_\ell(\mathbf{z}) = \{i \in [n] : z_i = \ell\}$ be the set of indices of nodes belonging to the ℓ^{th} cluster according to \mathbf{z} . For any subset $S \subseteq [n]$ and $\mathbf{x} = (x_1, \dots, x_n)^T \in \mathbb{R}^{n \times p}$, let $g(S | \mathbf{x})$ be a nonnegative function that measures the homogeneity of the covariates $\{x_i, i \in S\}$. That is, $g(S | \mathbf{x})$ takes larger values when all of the x_i with $i \in S$ are more similar. One can think of S as a potential cluster of nodes and $g(S | \mathbf{x})$ as a measure of the quality of such cluster, with regards the nodal information

Inspired by [18] and [20], we consider the following covariate-dependent random partition model:

$$(2.1) \quad p(\mathbf{z} | \mathbf{x}) \propto \prod_{\ell=1}^{L(\mathbf{z})} g(S_\ell(\mathbf{z}) | \mathbf{x}) \cdot c(S_\ell(\mathbf{z})) .$$

The non-negative function $S \mapsto c(S)$ is known as the cohesion function of the product partition probability model. In a random partition model based on the Dirichlet process, with baseline probability measure G_0 and concentration parameter α , one has $c(S) = \alpha(|S| - 1)!$ [7, 23].

Borrowing from [18], we define $g(S | \mathbf{x})$ based on an auxiliary probability model $q(\cdot | \cdot)$, where

$$(2.2) \quad g(S | \mathbf{x}) = \int \prod_{i \in S} q(x_i | \xi) \nu(\xi) d\xi .$$

Note that the covariates \mathbf{x} are not random. The term $\prod_{i \in S} q(x_i | \xi)$ measures the effect or contribution of the covariates on the prior probability of cluster S . One can choose $q(x_i | \xi)$ and $\nu(\xi)$ as a conjugate pair to facilitate the analytic evaluation of $g(S | \mathbf{x})$. For the cohesion function, we adopt $c(S) = \alpha(|S| - 1)!$.

Combining equations (2.1) and (2.2), we have

$$(2.3) \quad p(\mathbf{z} | \mathbf{x}) \propto \prod_{\ell=1}^{L(\mathbf{z})} \left[\int \prod_{i \in S_\ell(\mathbf{z})} q(x_i | \xi_\ell) d\nu(\xi_\ell) \right] c(S_\ell(\mathbf{z})) .$$

In this model, ξ_ℓ can be considered the center of the nodal covariates in cluster ℓ , and $q(x_i | \xi_\ell)$ a measure of how far the covariates in cluster S_ℓ are from its center ξ_ℓ . The model then averages over all possible centers $\xi_\ell \sim \nu$.

The distribution in (2.3) can be written as the marginal of

$$(2.4) \quad p(\mathbf{z}, \boldsymbol{\xi} | \mathbf{x}) \propto \prod_{\ell=1}^{L(\mathbf{z})} \left[c(S_\ell(\mathbf{z})) \prod_{i \in S_\ell(\mathbf{z})} q(x_i | \xi_\ell) \nu(\xi_\ell) \right] \cdot \prod_{\ell=L(\mathbf{z})+1}^{\infty} \nu(\xi_\ell) ,$$

where $\boldsymbol{\xi} = (\xi_1, \xi_2, \dots)$. One can use (2.4) to derive a Gibbs sampler for sampling the prior. To simplify the notation, we let

$$(2.5) \quad L = L(\mathbf{z}_{-i}) \quad \text{and} \quad S_\ell = S_\ell(\mathbf{z}_{-i})$$

for $\ell \in [L]$ denote the number of clusters of $\mathbf{z}_{-i} = (z_j, j \neq i)$ and the clusters themselves. Let

$$(2.6) \quad \psi_k := \begin{cases} |S_k| & k \in [L] \\ \alpha & k = L + 1 \end{cases} .$$

One can show that for $k \in [L + 1]$,

$$(2.7) \quad p(z_i = k, \xi_{L+1} | \mathbf{z}_{-i}, \boldsymbol{\xi}_{1:L}, \mathbf{x}) \propto \nu(\xi_{L+1}) \cdot \psi_k q(x_i | \xi_k) ,$$

where $\boldsymbol{\xi}_{1:L} = (\xi_1, \dots, \xi_L)$. This is equivalent to first drawing $\xi_{L+1} \sim \nu(\cdot)$, and then drawing z_i as follows:

$$(2.8) \quad p(z_i = k | \mathbf{z}_{-i}, \boldsymbol{\xi}_{1:L+1}, \mathbf{x}) \propto \psi_k q(x_i | \xi_k) .$$

As an example, for continuous features, we can take

$$(2.9) \quad q(x | \xi) = N(x; \xi, s^2 I) \quad \text{and} \quad \nu = N(0, \tau^2 I) ,$$

where $N(x; \xi, s^2 I)$ denotes the density of a normal distribution with mean ξ and covariance matrix $s^2 I$, evaluated at x . Then, $k \mapsto q(x_i | \xi_k)$ in (2.8) will be proportional to $\exp(-\|x_i - \xi_k\|^2 / 2s^2)$, which shows that if ξ_ℓ is the closest to x_i among $\{\xi_k\}$, then the inclusion of the covariate information increases the chance of assigning z_i to cluster ℓ .

An alternative approach to sample from the prior is to perform Gibbs sampling on the marginalized distribution (2.3). This leads to the following updates. For each $k \in [L + 1]$,

$$(2.10) \quad p(z_i = k | \mathbf{z}_{-i}, \mathbf{x}) \propto \psi_k \frac{g(S_k \cup \{i\} | \mathbf{x})}{g(S_k | \mathbf{x})} ,$$

where $S_{L+1} = \emptyset$ and $g(\emptyset | \mathbf{x}) = 1$. This approach is, in particular, useful when $q(\cdot | \cdot)$ and $\nu(\cdot)$ are conjugate so that $g(S | \mathbf{x})$ is easy to compute.

As another example, for categorical covariates, one can choose $q(x_i | \xi_k)$ to be a multinomial distribution and $\nu(\cdot)$ to be a Dirichlet distribution. Suppose there are R categorical features and the r th feature has a_r categories for $r = 1, \dots, R$. Then $x_i = (x_{i1}, \dots, x_{iR})$, where x_{ir} is the r -th feature of node i , and $x_{ir} \in \{1, \dots, a_r\}$. Each ξ_k collects parameters of R multinomial vectors, that is, $\xi_k = (\xi_{rk})_{r=1}^R$, where the coordinates $\xi_{rk} = (\xi_{rk}^1, \xi_{rk}^2, \dots, \xi_{rk}^{a_r})$ are independent draws from $\text{Dir}(\gamma \mathbf{1}_{a_r})$. We have

$$(2.11) \quad q(x_i | \xi_k) = \prod_{r=1}^R \prod_{c=1}^{a_r} (\xi_{rk}^c)^{1\{x_{ir}=c\}} \quad \text{and} \quad \nu = \prod_{i=1}^R \text{Dir}(\gamma \mathbf{1}_{a_r}) .$$

We usually take $\gamma = 1$.

With the priors thus defined, the network is assumed to follow a block model. Specifically,

$$(2.12) \quad P(A | \mathbf{z}) = \prod_{1 \leq i < j \leq n} \eta_{z_i, z_j}^{A_{ij}} (1 - \eta_{z_i, z_j})^{1 - A_{ij}} ,$$

where $\boldsymbol{\eta} = (\eta_{\ell m})_{1 \leq \ell, m \leq L}$ is the block matrix in a stochastic block model with $\eta_{\ell m}$ representing the link probability between a node from cluster ℓ and a node from cluster m . It is possible to obtain closed forms for the full conditional distributions of the unknown model parameters $\boldsymbol{\eta}$, \mathbf{z} , and $\boldsymbol{\xi}$ with appropriate choices of $q(\cdot)$ and $\nu(\cdot)$.

2.1. Gibbs sampler. We now derive a Gibbs sampler to sample from the complete posterior distribution of $(\mathbf{z}, \boldsymbol{\xi}, \boldsymbol{\eta})$ given A and \mathbf{x} . The main challenge is deriving the updates for \mathbf{z} .

We sample from \mathbf{z} , $\boldsymbol{\xi}$, and $\boldsymbol{\eta}$ through their full conditional distributions, which are given below, until reaching convergence, and then obtain a sample of adequate size of the posterior distribution for inference.

2.1.1. Initialization. We initialize the labels by drawing from a Chinese Restaurant Process (CRP),

$$\mathbf{z} \sim \text{CRP}(\alpha) .$$

A CRP can be seen as a special case of our prior without any covariates. This follows from (2.10) by setting $g(S | \mathbf{x}) = 1$. Once \mathbf{z} is initialized, all the other parameters can be initialized by the Gibbs updates derived below.

Note that initializing the chain by sampling \mathbf{z} from a CRP provides a random start without having to specify the number of the communities K . In many algorithms, spectral clustering is often used to initialize \mathbf{z} . For a Bayesian model, this is not a natural choice. Moreover, it requires the knowledge or an estimate of K .

2.1.2. Sampling \mathbf{z} . Let $b(x; a, b) = x^{a-1}(1-x)^{b-1}$ and for simplicity, define

$$(2.13) \quad \tilde{c}_\ell(S) := c(S) \prod_{j \in S} q(x_j | \xi_\ell) \nu(\xi_\ell) .$$

Note that $\tilde{c}_\ell(S)$ implicitly depends on ξ_ℓ . We have

$$\begin{aligned} p(A, \mathbf{z}, \boldsymbol{\xi}, \boldsymbol{\eta} | \mathbf{x}) &= p(A | \boldsymbol{\eta}, \mathbf{z}) \cdot p(\mathbf{z}, \boldsymbol{\xi} | \mathbf{x}) \cdot p(\boldsymbol{\eta}) \\ &\propto \prod_{1 \leq i < j \leq n} \eta_{z_i, z_j}^{A_{ij}} (1 - \eta_{z_i, z_j})^{1 - A_{ij}} \prod_{\ell=1}^{\infty} \tilde{c}_\ell(S'_\ell) \prod_{1 \leq m \leq \ell \leq \infty} b(\eta_{\ell m}; \beta, \beta) . \end{aligned}$$

Here, $S'_\ell = \{i \in [n] : z_i = \ell\}$ is the ℓ th community of \mathbf{z} . We assume that \mathbf{z} has L' communities $S'_1, S'_2, \dots, S'_{L'}$ and let $S'_{L'+1} = S'_{L'+2} = \dots = \emptyset$. The convention is that $c(\emptyset) = 1$ while $c(S) = \alpha \Gamma(|S|)$ when S is nonempty. Similarly, $\prod_{j \in \emptyset} (\dots) = 1$. In the above, we assume that $\boldsymbol{\xi} = (\xi_1, \xi_2, \dots)$ collects all possible ξ_ℓ and similarly for $\boldsymbol{\eta} = (\eta_{\ell m} : \ell, m \in \mathbb{N})$.

Fix i and let $S_\ell = \{j \in [n] \setminus i : z_j = \ell\}$ be the ℓ th community of \mathbf{z}_{-i} . We assume that \mathbf{z}_{-i} has L communities S_1, S_2, \dots, S_L and by convention, let $S_{L+1} = S_{L+2} = \dots = \emptyset$. To get the communities of \mathbf{z} from \mathbf{z}_{-i} , we either update S_k to $S'_k = S_k \cup \{i\}$ for some $k \in [L]$, or update S_{L+1} to $S'_{L+1} = S_{L+1} \cup \{i\} = \{i\}$, generating a new community. With the convention we use, we can compactly write both cases as $S'_k = S_k \cup \{i\}$ for all $k \in [L+1]$.

For any $k \in [L+1]$, we obtain

$$(2.14) \quad p(z_i = k, \boldsymbol{\xi}_{L+1}, \boldsymbol{\eta}_{L+1, [L]} \mid \mathbf{z}_{-i}, A, \boldsymbol{\xi}_{[L]}, \boldsymbol{\eta}_{[L], [L]}, \mathbf{x}) \propto \prod_{j:j \neq i} \eta_{k, z_j}^{A_{ij}} (1 - \eta_{k, z_j})^{1-A_{ij}} \cdot \frac{\tilde{c}_k(S_k \cup \{i\})}{\tilde{c}_k(S_k)} \prod_{\ell=1}^{L+1} \tilde{c}_\ell(S_\ell) \prod_{1 \leq m \leq \ell \leq L+1} b(\eta_{\ell m}; \beta, \beta) .$$

Letting

$$(2.15) \quad O_{i\ell} = \sum_{j:j \neq i} A_{ij} 1\{z_j = \ell\}, \quad n_\ell = \sum_{j:j \neq i} 1\{z_j = \ell\} ,$$

we have $\prod_{j:j \neq i} \eta_{k, z_j}^{A_{ij}} (1 - \eta_{k, z_j})^{1-A_{ij}} = \prod_{\ell=1}^L \eta_{k\ell}^{O_{i\ell}} (1 - \eta_{k\ell})^{n_\ell - O_{i\ell}}$.

Noting that $\prod_{\ell=1}^L \tilde{c}_\ell(S_\ell)$ is a constant in (2.14), and similarly for any term in

$$\prod_{1 \leq m \leq \ell \leq L+1} b(\pi_{\ell m}; \beta, \beta)$$

that does not have an index equal to $L+1$, we obtain

$$(2.16) \quad p(z_i = k, \boldsymbol{\xi}_{L+1}, \boldsymbol{\eta}_{L+1, [L]} \mid \mathbf{z}_{-i}, A, \boldsymbol{\xi}_{[L]}, \boldsymbol{\eta}_{[L], [L]}, \mathbf{x}) \propto \prod_{\ell=1}^L \eta_{k\ell}^{O_{i\ell}} (1 - \eta_{k\ell})^{n_\ell - O_{i\ell}} \cdot \frac{\tilde{c}_k(S_k \cup \{i\})}{\tilde{c}_k(S_k)} \tilde{c}_{L+1}(S_{L+1}) \prod_{m=1}^L b(\eta_{L+1, m}; \beta, \beta) .$$

The product over m runs up to L since only $\eta_{L+1, [L]}$ is a variable while $\eta_{L+1, L+1}$ is a constant. This is because z_i can take the new value $L+1$ but z_j with $j \neq i$ takes values in $[L]$, hence we do not need to sample $\eta_{L+1, L+1}$ at this stage.

Since $S_{L+1} = \emptyset$, we have

$$\begin{aligned} \tilde{c}_{L+1}(S_{L+1}) &= \nu(\xi_{L+1}) , \\ \tilde{c}_{L+1}(S_{L+1} \cup \{i\}) &= \alpha \Gamma(1) q(x_i \mid \xi_{L+1}) \nu(\xi_{L+1}) . \end{aligned}$$

Hence for $k \in [L+1]$,

$$\frac{\tilde{c}_k(S_k \cup \{i\})}{\tilde{c}_k(S_k)} \tilde{c}_{L+1}(S_{L+1}) = \nu(\xi_{L+1}) \psi_k q(x_i \mid \xi_k) ,$$

where ψ_k is defined in (2.6). Thus, we can compactly write

$$(2.17) \quad p(z_i = k, \boldsymbol{\xi}_{L+1}, \boldsymbol{\eta}_{L+1,[L]} \mid \mathbf{z}_{-i}, A, \boldsymbol{\xi}_{[L]}, \boldsymbol{\eta}_{[L],[L]}, \mathbf{x}) \propto \nu(\xi_{L+1}) \prod_{m=1}^L b(\eta_{L+1,m}; \beta, \beta) \cdot \psi_k q(x_i \mid \xi_k) \prod_{\ell=1}^L \eta_{k\ell}^{O_{i\ell}} (1 - \eta_{k\ell})^{n_\ell - O_{i\ell}} .$$

This is equivalent to the following. First draw $\xi_{L+1} \sim \nu$ and $\eta_{L+1,m} \sim \text{Beta}(\beta, \beta)$ for $m \in [L]$, all independently. Then draw z_i from

$$p(z_i = k \mid \mathbf{z}_{-i}, A, \boldsymbol{\xi}_{[L+1]}, \boldsymbol{\eta}_{[L+1],[L]}, \mathbf{x}) \propto \psi_k q(x_i \mid \xi_k) \prod_{\ell=1}^L \eta_{k\ell}^{O_{i\ell}} (1 - \eta_{k\ell})^{n_\ell - O_{i\ell}} .$$

For continuous features, we use (2.9) for $q(\cdot \mid \cdot)$ and ν , and for categorical variables we use (2.11) in the above updates.

2.1.3. *Sampling $\boldsymbol{\xi}$.* We have

$$p(\boldsymbol{\xi} \mid A, \mathbf{z}, \mathbf{x}, \boldsymbol{\eta}) = p(\boldsymbol{\xi} \mid \mathbf{z}, \mathbf{x}) \propto \prod_{\ell=1}^{L'} H_{S'_\ell}(\xi_\ell) ,$$

where H_S is the distribution with density

$$(2.18) \quad H_S(\xi) \propto \prod_{i \in S} q(x_i \mid \xi) \nu(\xi) .$$

That is, ξ_ℓ are independent draws from $H_{S'_\ell}$. We recall that $S'_\ell = \{i \in [n] : z_i = \ell\}$.

The details of sampling $\boldsymbol{\xi}$ are slightly different given different choices of $q(\cdot)$ and $\nu(\cdot)$ depending on whether continuous or categorical features are available. For continuous features with the Gaussian choice (2.9), $H_S(\xi) \propto \prod_{i \in S} N(x_i; \xi, s^2 I) \cdot N(\xi; 0, \tau^2 I)$ which gives

$$H_S = N\left(\frac{\tau^2 \sum_{i \in S} x_i}{|S|\tau^2 + s^2}, \frac{s^2 \tau^2}{|S|\tau^2 + s^2} I\right) .$$

For the categorical features with the choice (2.11), we have

$$H_S(\xi) \propto \prod_{i \in S} \prod_{r=1}^R \prod_{c=1}^{a_r} (\xi_r^c)^{1\{x_{ir}=c\}} \cdot \prod_{r=1}^R \prod_{c=1}^{a_r} (\xi_r^c)^{\gamma-1} = \prod_{r=1}^R \prod_{c=1}^{a_r} (\xi_r^c)^{\alpha_r^c(S)-1} ,$$

where $\alpha_r^c(S) := \gamma + \sum_{i \in S} 1\{x_{ir} = c\}$. That is, H_S is the product of Dirichlet distributions,

$$H_S = \prod_{r=1}^R \text{Dir}(\alpha_r^1(S), \dots, \alpha_r^{a_r}(S)) .$$

2.1.4. *Sampling $\boldsymbol{\eta}$.* Let us define the index sets

$$(2.19) \quad \Gamma_{k\ell} = \begin{cases} \{(i, j) : 1 \leq i < j \leq n\} & k = \ell \\ \{(i, j) : 1 \leq i \neq j \leq n\} & k \neq \ell \end{cases},$$

and block counts

$$(2.20) \quad M_{k\ell} = \sum_{(i,j) \in \Gamma_{k\ell}} A_{ij} 1\{z_i = k, z_j = \ell\} \quad \text{and} \quad N_{k\ell} = \sum_{(i,j) \in \Gamma_{k\ell}} 1\{z_i = k, z_j = \ell\} .$$

Then, we have

$$p(\boldsymbol{\eta} \mid A, \mathbf{z}, \mathbf{x}, \boldsymbol{\xi}) = p(\boldsymbol{\eta} \mid A, \mathbf{z}) \propto \prod_{k < \ell} \eta_{k\ell}^{M_{k\ell} + \beta - 1} (1 - \eta_{k\ell})^{N_{k\ell} - M_{k\ell} + \beta - 1} .$$

Thus, $\eta_{k\ell}$ are independent draws from $\text{Beta}(M_{k\ell} + \beta, N_{k\ell} - M_{k\ell} + \beta)$.

3. SIMULATION STUDY

In this section, we carry out multiple simulation studies in which we compare our methods, which we refer to as BCDC (Bayesian community detection for networks with covariates), with i) the covariate-assisted spectral clustering (CASC) algorithm [5], which uses both the network and the covariates information in a spectral clustering algorithm, ii) k -means algorithms (k -means) applied only to the covariates, iii) spectral-clustering (SC) of the adjacency matrix, and iv) a Bayesian SBM (BSBM), which is essentially a special case of our model with $g(S \mid \mathbf{x}) = 1$, therefore utilizing only the network information. For CASC, the core idea is to first construct a new Laplacian matrix $L_x = L + \tau X X^T$, where L is the Laplacian matrix for the network and X denotes the n by p feature matrix, and then apply the standard spectral clustering algorithm on L_x . Throughout, we select τ based on the automated procedure given in [5, Section 2.3].

We consider simulation designs with (a) continuous features, (b) discrete or categorical features, and (c) high-dimensional features with networks simulated from stochastic block models with varying connectivity patterns and sparsity levels. The performance of the estimated communities is measured by normalized mutual information (NMI), a measure ranging from 0 (random guessing) to 1 (perfect agreement).

Overall, the simulation studies show that our method consistently outperforms the competitors and demonstrates the gain of our model by utilizing both the network and nodal information for detecting the community structures. The code for these experiments is available at GitHub repository [aaamini/bcdc](https://github.com/aaamini/bcdc) [24].

3.1. Continuous covariates. We first consider simulated networks with continuous covariates, and in particular, the Gaussian setting (2.9). We generate networks from

an SBM having connectivity matrix $\eta = (\eta_{k\ell}) \in [0, 1]^{K \times K}$ with

$$(3.1) \quad \eta_{k\ell} = \begin{cases} p & k = \ell \\ rp & k \neq \ell \end{cases} .$$

The parameter $r \in [0, 1]$ controls the magnitude of disparity between the within and between connectivities and is a measure of network information for the community structure. In our simulations, we set $p = 0.1$ and vary r . We consider $n = 150$ nodes with $K = 2$ communities of 100 and 50 nodes, respectively.

For each node, we generate $d = 2$ features, with one *signal* feature related to the community structure and one *noise* feature whose distribution is the same for all nodes. Letting $x_i \in \mathbb{R}^2$ be the feature vector for node i and $e_1 = (1, 0)$, we take

$$x_i | z_i \sim N(\mu\sigma_{z_i}e_1, I_2) ,$$

where $\sigma_1 = +1$, $\sigma_2 = -1$ and $z_i \in \{1, 2\}$ is the community label of node i . Here $\mu \in [0, \infty)$ is proportional to the signal-to-noise ratio of the covariate information.

Figure 2 shows the boxplots of NMI from BCDC and competing methods, averaged over 28 replications, under different settings of r and μ . For BCDC, we have used parameters $\alpha = 10$, $\beta = 1$ and $\tau = s = 1$, and ran the sampler for 1000 iterations. Note that in our comparison, all of the competing methods were given an additional advantage by assuming the knowledge of the true number of communities. However, our method (red) consistently outperforms these other methods. An interesting notable case is that of high network information ($r = 0.3$) and pure noise covariate information ($\mu = 0$). In this case, BCDC performs as well as BSBM which only operates on network information, while CASC performs much worse being misled by pure noise covariates.

3.2. Categorical covariates. We next consider a simulation study for networks with categorical covariates. For each node i , we again generate $d = 2$ features with one *signal* feature related to the community structure and one *noise* feature whose distribution is the same for all nodes. We consider two designs:

(1) We consider networks with $n = 150$ nodes and $K = 3$ equally-sized communities. The signal features are taken to be the true community labels and the noise features are uniformly distributed on $\{1, 2, 3\}$.

(2) We consider networks with $n = 150$ nodes and $K = 2$ communities of 100 and 50 nodes. We create two 4-category features. Let $x_i = (x_{i1}, x_{i2}) \in \{1, 2, 3, 4\}^2$ be the feature vector for node i . We use the following generative model

$$\begin{aligned} \theta_1, \theta_2 &\sim \text{Dir}(\mathbf{1}_4) , \\ x_{i1} | z_i &\sim \theta_{z_i}, \quad x_{i2} | z_i \sim \mathbf{1}_4/4 , \end{aligned}$$

where, for example, $x_{i1} \sim \theta_{z_i}$ means that x_{i1} is a categorical variable with probability vector θ_{z_i} .

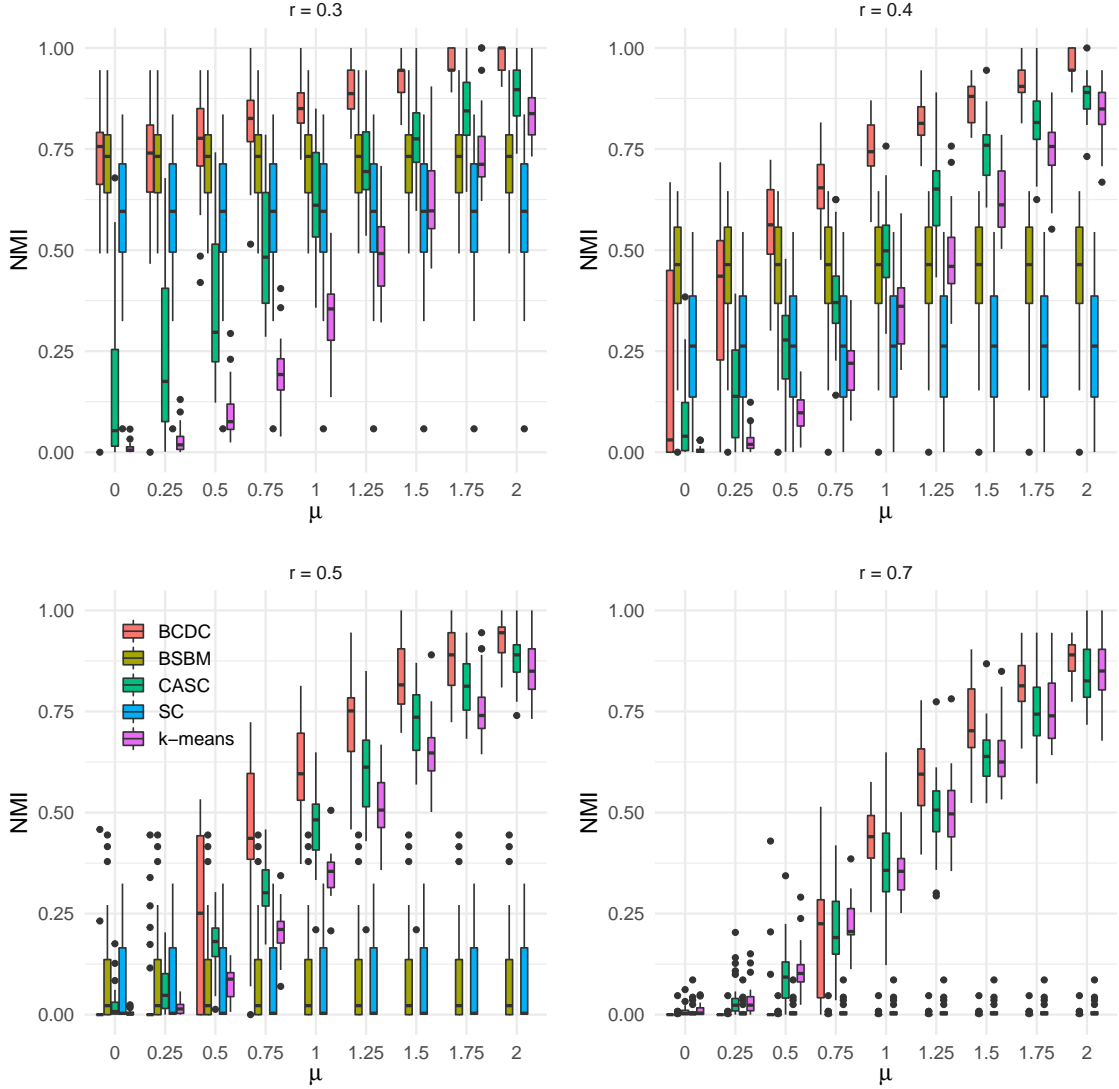


FIGURE 2. Boxplots of NMI for five different methods on a 2-block SBM with continuous data. In all cases, $p = 0.1$, and we vary the network and covariate signal-to-noise ratios, r and μ , respectively.

In both cases, we use an SBM with connectivity (3.1), setting $p = 0.1$ and varying r from 0.1 to 0.8. For the parameters of our model, we again set $\alpha = 10$, and ran the chain for 1,500 iterations. As above, the results are given over 28 replicates.

Figure 3 shows the boxplots of NMI as a function of r (the network information measure) under the two covariate designs. Once again, all methods except BCDC were given the true number of communities. The NMI values obtained under the proposed model are generally higher than those of the other models with a slightly

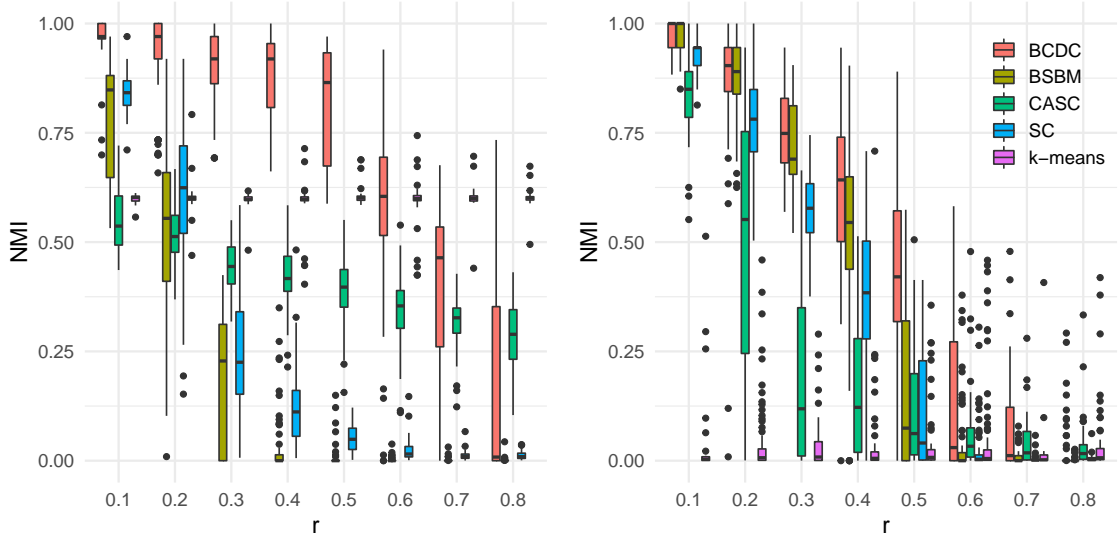


FIGURE 3. Boxplots of NMI for five different methods on a 3-block (left) and 2-block (right) SBM with categorical data.

larger variance, which is likely due to the additional uncertainty in estimating the number of the communities.

3.3. Sparse networks and high-dimensional features. Finally, we consider a setting from [29], who proposed a covariate-regularized procedure for community detection in sparse graphs. This allows us to explore whether our model works for sparse networks, as well as networks with high-dimensional features. We consider the exact simulation setting as in [29], in which the networks are generated from a 3-block SBM on 800 nodes with block-size ratios 3 : 4 : 5. The true connectivity matrix is

$$B = 0.01 \begin{bmatrix} 1.6 & 1.2 & 0.16 \\ 1.2 & 1.6 & 0.02 \\ 0.16 & 0.02 & 1.2 \end{bmatrix},$$

leading to a very sparse network, with expected average degree ≈ 5.8 . The covariates are generated from 100-dimensional Gaussian distributions $N(\mu_{z_i}, I_{100})$, with centers that are only non-zero on the first two dimensions:

$$\mu_1 = (0, 2, \mathbf{0}_{98}), \quad \mu_2 = (-1, -0.8, \mathbf{0}_{98}), \quad \mu_3 = (1, -0.8, \mathbf{0}_{98}).$$

In this setting, it is difficult to distinguish clusters 1 and 2 using the network information alone, and clusters 2 and 3 based on nodal covariates alone.

This experiment was repeated 28 times for independently generated samples. In each replicate, we ran the chain for 1,000 iterations. The boxplots of the results are shown in Figure 4. Note that our method consistently achieves a better NMI than all of the other methods. Although we did not carry out a direct comparison with the method

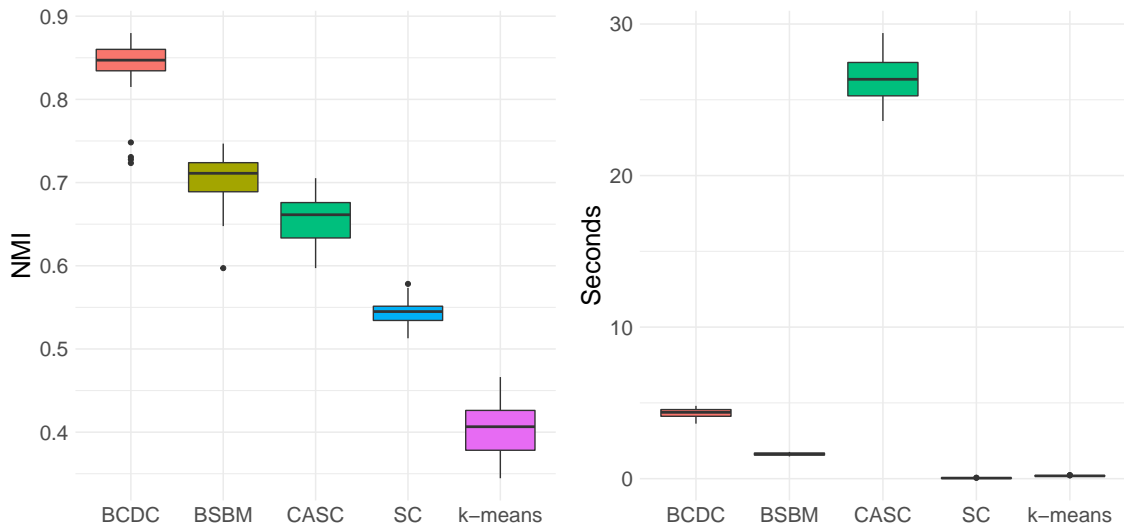


FIGURE 4. Boxplots of NMI (left) and run time (right) for five different methods when the network is sparse and the covariates are high-dimensional.

from [29] since their work focuses on regularizing high-dimensional features, our NMI results are stable and seem to be higher than those reported in [29]. Importantly, we also see in Figure 4 that BCDC is only slightly slower than all of the methods that use only the network or only the covariates, but is considerably faster than CASC, which also uses both the network and the nodal information. This illustrates the disadvantage of CASC for larger sparse networks and highlights the efficiency of our MCMC algorithm. That CASC slows down for larger networks can be attributed to the addition of the dense τXX^T to the sparse Laplacian L , resulting in an overall dense similarity matrix L_x .

4. REAL DATA ANALYSIS

In this section, we apply our model to the same two datasets from [29], a network representing Mexican political elites and a network representing the Weddell Sea ecosystem. We compare our the results from our models against several methods that use only the network, only the covariates, and both the network and covariates. The code is available at GitHub repository [aaamini/bcdc](https://github.com/aaamini/bcdc) [24].

4.1. Performance measures. In addition to computing the NMI with the (alleged) ground truth labels, it is also helpful to compare the performance using the Bayesian information criterion (BIC) based on an SBM likelihood conditional on the labels. This is especially important because, unlike in the simulations, the “true” clusters are exogenously specified. The (conditional) BIC is defined as the log-marginal likelihood

multipled by -2 . That is,

$$(4.1) \quad \text{BIC}(\mathbf{z}) = -2 \log \int p(A \mid \boldsymbol{\eta}, \boldsymbol{\pi}, \mathbf{z}) d\boldsymbol{\eta} d\boldsymbol{\pi}$$

$$(4.2) \quad \approx -2 \log p(A \mid \hat{\boldsymbol{\eta}}, \hat{\boldsymbol{\pi}}, \mathbf{z}) + c(K) \log \binom{n}{2},$$

where K is the number of communities in \mathbf{z} , $c(K) = \frac{1}{2}K(K+1) + (K-1)$ is the degrees of freedom in the parameters $(\boldsymbol{\eta}, \boldsymbol{\pi})$, $\boldsymbol{\pi}$ is the label prior, and $(\hat{\boldsymbol{\eta}}, \hat{\boldsymbol{\pi}})$ is the maximum likelihood estimator of those parameters, i.e., the maximizer of $(\boldsymbol{\eta}, \boldsymbol{\pi}) \mapsto p(A \mid \boldsymbol{\eta}, \boldsymbol{\pi}, \mathbf{z})$. We assume a uniform prior over $\boldsymbol{\eta}$ and $\boldsymbol{\pi}$. Note that (4.2) is the well-known approximation to the BIC [22, 14] and it shows the usefulness of $\text{BIC}(\mathbf{z})$ as a measure of performance for real networks: due to the presence of the complexity term $\approx c(K) \log(n^2)$, we get a good balance of the model fit and the number of communities. Label vectors \mathbf{z} with smaller $\text{BIC}(\mathbf{z})$ are thus more desirable from a block modeling standpoint, regardless of their relation to the ground truth.

We have

$$p(A \mid \boldsymbol{\eta}, \boldsymbol{\pi}, \mathbf{z}) = \prod_{k \leq \ell} \eta_{k\ell}^{M_{k\ell}} (1 - \eta_{k\ell})^{N_{k\ell} - M_{k\ell}} \prod_k \pi_k^{n_k(\mathbf{z})},$$

where $n_k(\mathbf{z}) = \sum_i 1\{z_i = k\}$, and $M_{k\ell}$ and $N_{k\ell}$ are as in (2.20). Hence, the exact BIC in our setting is

$$\text{BIC}(\mathbf{z}) = -2 \left[\sum_{k \leq \ell} \log B(M_{k\ell} + 1, N_{k\ell} - M_{k\ell} + 1) + \log \mathbf{B}(\mathbf{n}(\mathbf{z}) + \mathbf{1}_K) \right],$$

where $\mathbf{n}(\mathbf{z}) = (n_k(\mathbf{z}))$ and $\mathbf{B}(\cdot)$ is the multivariate Beta function.

4.2. Mexican Political Elites. The first dataset we consider involves Mexican political elites [8]. In this network, the $n = 35$ vertices represent Mexican presidents and their close collaborators, and the 117 edges represent significant political, kinship, friendship, or business ties among them. The ground truth is a classification of the politicians according to their professional background: military and civilians. The covariate we include is the number of years since 1990 that the actor first got a significant governmental position. Figure 5 reveals that this covariate has some discriminatory power in the cluster labels. This is due to the fact that after the Mexican revolution at the beginning of the twentieth century, the political elite was dominated by the military, and later the civilians gradually succeeded the power.

Table 1 contains the NMI results of our method compared with the same comparison methods in the simulation section. We see that our method achieves the best results, and we visualize our estimated clusters in the network compared with the true labels in Figure 6. Again, for the other methods, we assume the knowledge of the true number of clusters while ours learns the number of the clusters via posterior inference for NMI comparisons.

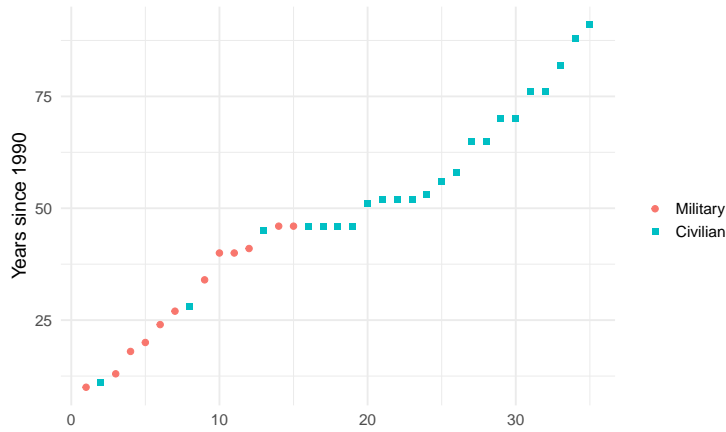


FIGURE 5. Node feature for the Mexican political network, which is the number of years since 1990 that the actor first got a significant governmental position.

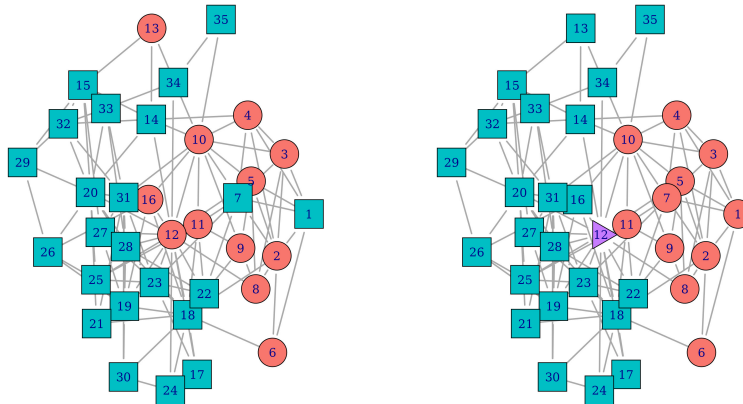


FIGURE 6. Mexican political network with nodes colored by true (left) and estimated (right) cluster labels.

As already pointed out in [29], node 35 has exactly one connection to each of the military and civilian groups, but obtained a governmental position in the 90s, which greatly hinted at a civilian background. By using the covariate, our method accurately captures this label. On the other hand, node 9 seized power in 1940 when the government was almost equally represented by civilian and military politicians, which makes detecting his group difficult, but has more edges to the military group

Dataset	BCDC	CASC	k -means	SC	BSBM
Mexican politicians	0.43	0.29	0.26	0.37	0.24
Weddell Sea	0.44	0.30	0.35	0.24	0.23

TABLE 1. NMI results on the two real datasets.

Dataset	“True”	BCDC	CASC	k -means	SC	BSBM
Mexican politicians	636	586	620	626	587	587
Weddell Sea	138k	33k	140k	144k	128k	71k

TABLE 2. BIC results on the two real datasets.

than the civilian group. In this case, our method correctly assigns the military label to it by considering the graph structure.

We also notice that node 1 has five connections to the military and only one connection to the civilian, and node 1 seized power in 1911. Similarly for node 7, which has five connections to the military and three connections to the civilian and seized power in 1928. For these nodes, both the network and the covariates strongly indicate a closer relationship to the military, which is what our method assigns despite the true label showing civilian. Finally, our method assigns node 12 to its own cluster. This is likely because this is the highest-degree node with 5 military connections and 12 civilian connections. However, in researching node 12, we discovered that Miguel Alemán Valdés was the first civilian president after several military presidents, which suggests that there may have been a labeling error in the original publication of this dataset from [8]. This could explain why our method has the best BIC, even better than the “true” labels, in Table 2.

4.3. Weddell Sea Ecosystem. The second dataset we consider is a predator-prey, directed network representing the marine food web of the Weddell Sea off of the Antarctic Peninsula, which was collected by [10]. Since ecosystems are complex, interconnected environments, network analyses have emerged as a popular technique for untangling these connections. The Weddell Sea network has 487 nodes that signify different marine species, and there is a link between nodes i and j if species i (predator) feeds on species j (prey). Following [29], we construct a binary, undirected network from this directed network in which $A_{ij} = 1$ if there are at least 5 common prey between species i and j , and $A_{ij} = 0$ otherwise. The network is shown in Figure 7.

In [10], the authors analyze the relationship between the body size of each species and its feeding type: primary producer, herbivorous/detrivorous, detrivorous, carnivorous,

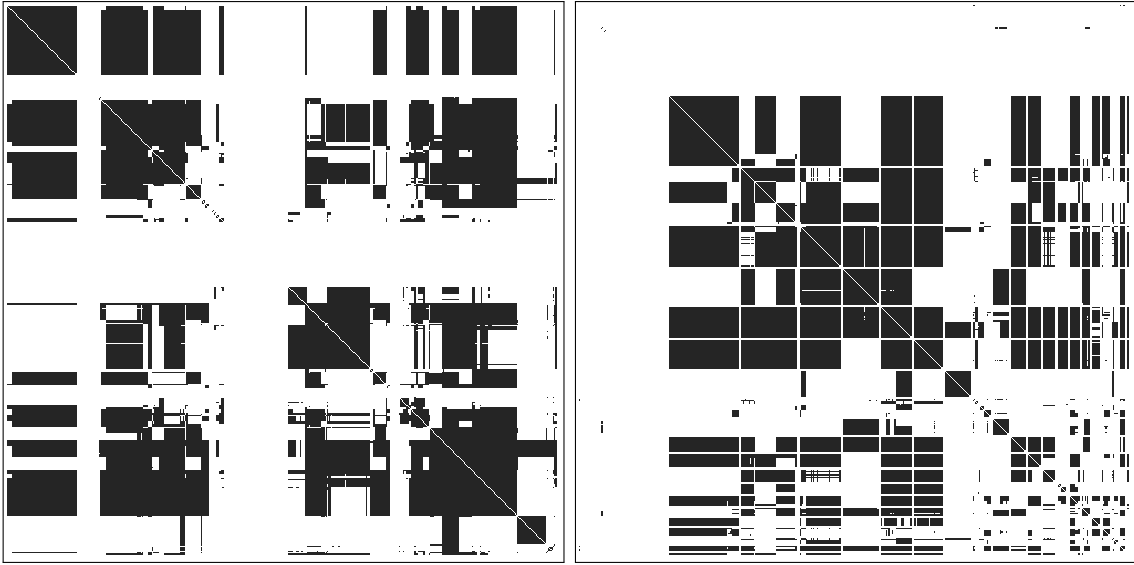


FIGURE 7. Visualization of the adjacency matrix for the Weddell Sea network clustered by the true feeding type (left) and estimated clusters (right). In each case, the rows and columns of the matrix are permuted so that nodes in the same cluster form contiguous blocks. Clusters on the right are ordered according to their size.

carnivorous/necrovorous, and omnivorous. Figure 1 shows these body sizes grouped by feeding type, where, again following [29], we group detritivorous, carnivorous, carnivorous/necrovorous as “Carnivore” to obtain four groups. The adjacency matrix in Figure 7 (left) is also sorted by these groups. The authors of [10] found body size to be positively correlated with trophic level, but noted that “predators on intermediate trophic levels do not necessarily feed on smaller or prey similar in size but depending on their foraging strategy have a wider prey size range available.” Therefore, body size is insufficient on its own to distinguish the groups, and it would be preferable to consider the interconnectedness of the food web when tasked with clustering the species.

Table 1 shows that BCDC provides the best clustering results compared to the other methods. Therefore, using all of the available information provides an improvement in clustering accuracy over the use of just the network structure or the nodal information. As before, BCDC is the only method that did not know that there are four “true” groups. Interestingly, BCDC estimates many more clusters – 21 in total – which may explain its higher NMI, since we see qualitatively in Figure 7 (right) a more refined block structure. This is quantified and corroborated through BIC in Table 2, which again shows our method outperforms even the “true” clusters. All of this suggests there may be distinct sub-blocks within the Herbivore, Carnivore, and Omnivore classes.

5. DISCUSSION

In this work, we proposed a Bayesian model for community detection in networks with covariates in which both the network and node features of the network are jointly utilized for estimating community structure. In particular, the contribution of nodal information is explicitly modeled in the prior distribution for the community labels via a covariate-dependent random partition prior. We proposed efficient MCMC algorithms for sampling the posterior distributions of all the parameters including the community labels and the number of the communities. Numerical studies demonstrated the overall superior performance of our model over many of the existing methods.

Compared to an almost exclusive literature of frequentist methods, our work is among the first in proposing a Bayesian approach for tackling the problem, which confers some notable advantages in terms of uncertainty quantification, as well as estimating all the model parameters. Notably, unlike the other methods in the literature, our model estimates the number of communities via posterior inference without any knowledge or prior information on the true number. Future work will be devoted to developing Bayesian models for community detection in degree-corrected SBMs and dynamic network models.

ACKNOWLEDGEMENT

LS and LL were supported by NSF grants DMS 2113642 and DMS 1654579. AA would like to acknowledge the support of NSF grant DMS-1945667. NJ was partially supported by NIH/NICHD grant 1DP2HD091799-01.

REFERENCES

- [1] Arash A. Amini and Elizaveta Levina. On semidefinite relaxations for the block model. *The Annals of Statistics*, 46(1):149 – 179, 2018.
- [2] Arash A. Amini, Marina S. Paez, and Lizhen Lin. Hierarchical Stochastic Block Model for Community Detection in Multiplex Networks. *arXiv e-prints*, page arXiv:1904.05330, March 2019.
- [3] Brian Ball, Brian Karrer, and MEJ Newman. Efficient and principled method for detecting communities in networks. *Physical Review E*, 84(3):036103, 2011.
- [4] Peter J. Bickel and Aiyu Chen. A nonparametric view of network models and newman girvan and other modularities. *Proceedings of the National Academy of Sciences of the United States of America*, 106(50):21068–21073, 2009.
- [5] Norbert Binkiewicz, Joshua T Vogelstein, and Karl Rohe. Covariate-assisted spectral clustering. *Biometrika*, 104(2):361–377, 2017.
- [6] Paul Erdős and Alfréd Rényi. On random graphs i. *Publicationes Mathematicae (Debrecen)*, 6:290–297, 1959.

- [7] Thomas S Ferguson. A Bayesian analysis of some nonparametric problems. *The annals of statistics*, pages 209–230, 1973.
- [8] Jorge Gil-Mendieta and Samuel Schmidt. The political network in mexico. *Social Networks*, 18(4):355–381, 1996.
- [9] Paul W Holland, Kathryn Blackmond Laskey, and Samuel Leinhardt. Stochastic blockmodels: First steps. *Social networks*, 5(2):109–137, 1983.
- [10] Ute Jacob, Aaron Thierry, Ulrich Brose, Wolf E Arntz, Sofia Berg, Thomas Brey, Ingo Fetzer, Tomas Jonsson, Katja Mintenbeck, Christian Möllmann, et al. The role of body size in complex food webs: A cold case. *Advances in ecological research*, 45:181–223, 2011.
- [11] Brian Karrer and M. E. J. Newman. Stochastic blockmodels and community structure in networks. *Phys. Rev. E*, 83:016107, Jan 2011.
- [12] E.D. Kolaczyk. *Statistical Analysis of Network Data: Methods and Models*. Springer Verlag, 2009.
- [13] Eric D. Kolaczyk, Lizhen Lin, Steven Rosenberg, Jackson Walters, and Jie Xu. Averages of unlabeled networks: Geometric characterization and asymptotic behavior. *The Annals of Statistics*, 48(1):514 – 538, 2020.
- [14] Sadanori Konishi and Genshiro Kitagawa. Information criteria and statistical modeling. 2008.
- [15] László Lovász. *Large Networks and Graph Limits*, volume 60. American Mathematical Society Providence, 2012.
- [16] Ulrike Von Luxburg. A tutorial on spectral clustering. *Statistics and Computing*, 17(4):395–416, 2007.
- [17] Morten Mørup and Mikkel N. Schmidt. Bayesian community detection. *Neural Comput.*, 24(9):2434–2456, September 2012.
- [18] Peter Müller and Fernando Quintana. Random partition models with regression on covariates. *Journal of statistical planning and inference*, 140(10):2801–2808, 2010.
- [19] M. E. J. Newman. Modularity and community structure in networks. *Proceedings of the National Academy of Sciences*, 103(23):8577–8582, 2006.
- [20] Ju-Hyun Park and David B Dunson. Bayesian generalized product partition model. *Statistica Sinica*, pages 1203–1226, 2010.
- [21] Karl Rohe, Sourav Chatterjee, and Bin Yu. Spectral clustering and the high-dimensional stochastic block model. *Annals of Statistics*, 39:1878–1915, 2011.

- [22] Gideon Schwarz. Estimating the dimension of a model. *The annals of statistics*, pages 461–464, 1978.
- [23] Jayaram Sethuraman. A constructive definition of dirichlet priors. *Statistica Sinica*, 4(2):639–650, 1994.
- [24] Luyi Shen, Arash A. Amini, Nathaniel Josephs, and Lizhen Lin. BCDC model for community detection with node covariates. <https://github.com/aaamini/bcdc>, 2022.
- [25] Tracy M. Sweet. Incorporating Covariates Into Stochastic Blockmodels. *Journal of Educational and Behavioral Statistics*, 40(6):635–664, December 2015.
- [26] Christian Tallberg. A bayesian approach to modeling stochastic blockstructures with covariates. *The Journal of Mathematical Sociology*, 29(1):1–23, 2004.
- [27] Haolei Weng and Yang Feng. Community detection with nodal information: Likelihood and its variational approximation. *Stat*, 11, 2022.
- [28] P. J. Wolfe and S. C. Olhede. Nonparametric graphon estimation. *ArXiv e-prints*, September 2013.
- [29] Bowei Yan and Purnamrita Sarkar. Covariate regularized community detection in sparse graphs. *Journal of the American Statistical Association*, 116(534):734–745, 2021.
- [30] Yuan Zhang, Elizaveta Levina, Ji Zhu, et al. Community detection in networks with node features. *Electronic Journal of Statistics*, 10(2):3153–3178, 2016.
- [31] Yun Zhang, Kehui Chen, Allan Sampson, Kai Hwang, and Beatriz Luna. covariate adjusted stochastic block model. *Journal of Computational and Graphical Statistics*, 28(2):362–373, 2019.

LUYI SHEN, DEPARTMENT OF APPLIED AND COMPUTATIONAL MATHEMATICS AND STATISTICS,
THE UNIVERSITY OF NOTRE DAME

Email address: lshen4@nd.edu

ARASH AMINI, DEPARTMENT STATISTICS, UCLA

Email address: aaamini@ucla.edu

NATHANIEL JOSEPHS, DEPARTMENT OF BIostatISTICS, YALE SCHOOL OF PUBLIC HEALTH

Email address: nathaniel.josephs@yale.edu

LIZHEN LIN, DEPARTMENT OF APPLIED AND COMPUTATIONAL MATHEMATICS AND STATISTICS,
THE UNIVERSITY OF NOTRE DAME

Email address: lizhen.lin@nd.edu